Metrol. Meas. Syst., Vol. 32 (2025) No. 1, pp. 1–15
DOI: 10.24425/mms.2025.152781

PAN POLSKA AKADEMIA NAUK

METROLOGY AND MEASUREMENT SYSTEMS
Index 330930, ISSN 0860-8229
www.metrology.wat.edu.pl

M&MS

INDIRECT SIMULTANEOUS EDDY-CURRENT MEASUREMENTS OF SUBSURFACE PROFILES OF ELECTROPHYSICAL PROPERTIES IN PLANAR OBJECTS USING A PRIORI KNOWLEDGE ABOUT THEM

Volodymyr Ya. Halchenko, Ruslana Trembovetska, Volodymyr Tychkov

Cherkasy State Technological University, Instrumentation, Mechatronics and Computer Technologies Department, Blvd. Shevchenkà, 460, 18006, Cherkasy, Ukraine (✉ *v.tychkov@chdtu.edu.ua*)

Abstract

An eddy-current method of simultaneous indirect measurements of distributions of electrical conductivity and magnetic permeability in the subsurface zone of planar objects is proposed, based on a surrogate optimization algorithm using neural network metamodels of reduced dimensionality. Reduction of their dimensions and the space for finding an extremum is performed using the Kernel PCA method, which involves nonlinear transformations as a result of computational operations with the Gaussian kernel function. The construction of metamodels involved the use of deep learning methods. The peculiarities of metamodels include the performance of two functions, in particular, providing low-cost efficient computing and accumulating additional *a priori* information about the measurement process, which is digitally entered into the design of the experiment determining the training samples for training of deep neural networks. Taken as a whole, it made it possible to achieve higher accuracy characteristics of indirect measurements.

Keywords: Indirect measurements, electrophysical property profiles, surrogate optimization, reduced dimension metamodel.

1. Introduction

Eddy current technology is often used to indirectly measure the electrophysical properties of conductive materials [1–3]. Determination of distributions of *electrical conductivity* (EC) and *magnetic permeability* (MP) in the subsurface layers of a material provides a significant amount of information about features of the microstructural state of the *test objects* (TO). Thus, this makes it possible to monitor the quality of various technological operations in the production process and correct them throughout the entire manufacturing cycle of industrial products. The structural sensitivity of the EC and MP profiles is an important factor in the considerable interest of researchers in improving methods for selecting such information from the results of direct measurements of EMF by *eddy current probes* (ECPs) during non-destructive testing of objects, since it is impossible to obtain it directly. The desired subsurface distributions of electrophysical

Article history: received June 24, 2024; revised October 15, 2024; accepted October 29, 2024; available online February 10, 2025.

properties of materials depend on the parameters of the primary probes used, the geometry of the TO, and the laws of physics, which establish complex relationships with the measured values of the ECP, *i.e.*, the amplitude and phase of the EMF. The methods above are computational procedures that, as a result of processing the data obtained by the probes according to certain algorithms, lead to establishment of the required profiles of electrophysical properties of materials with a certain accuracy. It is desirable to simultaneously determine both profiles without application of technically complex measuring equipment, *i.e.*, at one fixed frequency of excitation of the electromagnetic field of the object being sensed. For mathematical reasons, these problems belong to the class of inverse problems, the solution of which causes significant difficulties due to the peculiarities of their belonging to the incorrectly posed ones [4]. Researchers propose various theoretical approaches and computational techniques to improve methods for determining the profiles of EC and MP, in particular, those mentioned in recent publications [5–10]. In articles [11, 12], the authors provide a critical analysis of the methods proposed in them and a fairly detailed generalization of the observed trends in their development, as well as further directions for their improvement. In particular, the authors point out the prospects of combining the advantages of optimization and data-driven methods in one computational algorithm, which was implemented while using a surrogate optimization method [13] with reduced-dimensional metamodels implemented on deep MLP-neural networks. It should be noted that this involved a preliminary reduction of dimensionality of the metamodels and, accordingly, the search space of the optimization algorithm using linear transformations with the principal components method of PCA. This made it possible to significantly reduce the requirements for computational and time resources for solving these problems, since without this technique they required much more space, while providing even worse accuracy in determining the profiles.

In addition, when solving inverse problems, the involvement of additional *a priori* information about the course of the profile measurement process in the computation is of significant, if not decisive, importance, which makes it possible to obtain a more accurate solution to the problem. Under conditions of solution instability, which is typical for inverse problems, ignoring this rule does not allow us to localize the desired solution in conditions of its non-uniqueness, and therefore leads to a loss of accuracy. From now on, we will consider *a priori* information to be information that is obtained regardless of the measurement results. Usually, to introduce *a priori* information into the computational process, a mathematical model is supplemented with appropriate additional relations and connections that the solution must satisfy and that describe its fine structure, highlighting its physical essence. When solving any inverse problem, such individual *a priori* information always exists. In the mentioned studies of the authors [11, 12], a form of *a priori* information different from the traditional one was used. Its input into neural network surrogate models, *i.e.*, metamodels, was performed digitally, due to homogeneous multifactorial computerized *designs of experiments* (DOEs) [14, 15]. It is the digital data at the point of the design of the experiment, together with the values of the ECP EMF calculated therein that are used as training samples for training deep neural networks and allow us to establish, due to their unique generalizing properties, subtle, complex, and significantly nonlinear patterns of ECP signal formation hidden in the data. *A priori* information can be complete or incomplete, which is also acceptable, simplifying the preparation of metamodels. An increase in its volume leads to an increase in the transparency of the physics of the measurement process, thus surrogate models will provide better opportunities for solving the inverse problem.

Summarizing, it should be noted that the literature review of recent research on the analysed topic has not revealed the existence of effective methods for solving the problems of indirect measurements of EC and MP profiles, taking into account the available *a priori* knowledge of the desired solutions in this specific form. It is also advisable to conduct research aimed at further

Metrol. Meas. Syst., Vol. 32 (2025), No. 1, pp. 1–15
DOI: 10.24425/mms.2025.152781

reduction of the dimensions of surrogate models, which is promising with the use of nonlinear transformations with much greater possibilities for this.

Therefore, the aim of the paper is to develop a method for indirect simultaneous eddy current measurements of subsurface profiles of electrical conductivity and magnetic permeability of planar objects using a surrogate optimization algorithm and neural network metamodels of the dimensionality reduced by nonlinear Kernel PCA transformations and accumulating additional *a priori* knowledge about the desired solution, increasing the completeness of such information, which combines a full-scale experiment, direct modelling, and the inverse part to achieve high accuracy characteristics.

2. Research methodology

Measurements of the EC and MP profiles are performed in stages according to the scheme shown in Fig. 1. The profiles are continuous along the thickness of the material, but we will consider them discretized in the following as a result of a piecewise constant approximation. A solution to the problem may be done in the form of a vector, as shown in Fig. 1.

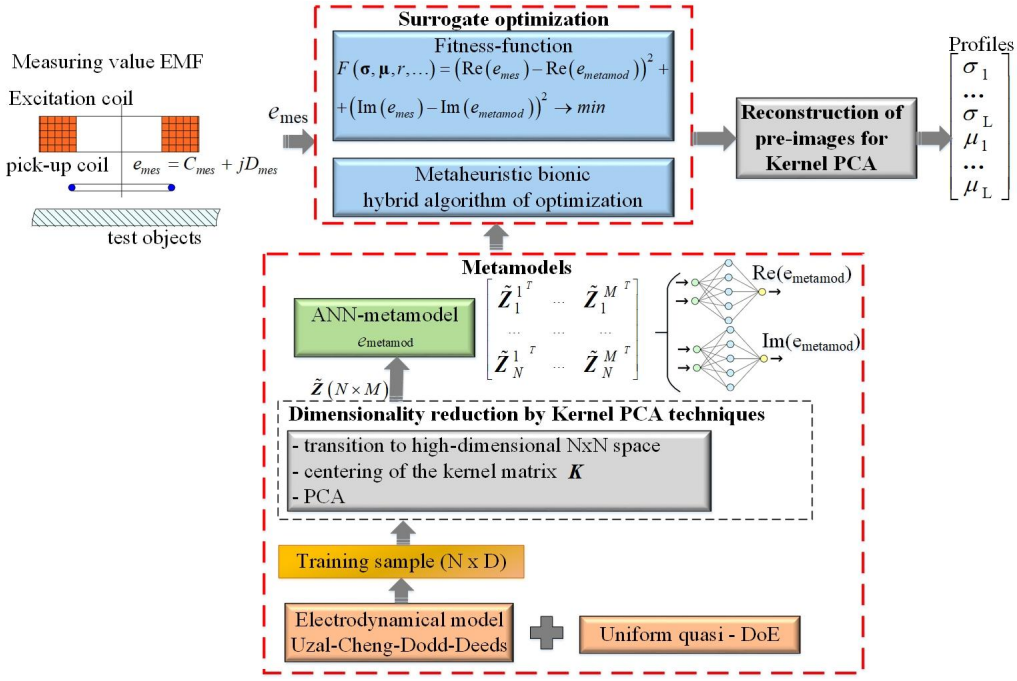

Fig. 1. Main stages of the technique of indirect eddy current measurements of the subsurface profiles of EC and MP.

A detailed description of the stages of measuring the electrophysical properties of the TO has already been given by the authors in previous published studies, in particular in [11, 12], so their essence is briefly recalled here. However, this article, offers certain changes in the content of some stages, the description of which is given more attention to in the future.

Hence, first, the EMF e_{mes} is measured by a surface ECP located above the planar TO. Second, the obtained measurement result in the form of the EMF amplitude and phase is sent for processing

to the surrogate optimization unit where the metaheuristic algorithm of global search for an extremum, using a fitness function with a component in the form of a metamodel, minimizes the difference between the measured and theoretical values of the EMF by varying the values of electrophysical parameters and finds the desired profiles in a reduced space. Third, a metamodel is preliminarily created to be used at the second stage of calculations, which is actually a neural network solution to the direct problem of determining the theoretical model value of the EMF, but it is characterized by a high computational efficiency and low resource consumption. In contrast to the solution scheme given in [11], which illustrates actions in a full-factor space, *i.e.*, uses a full-dimensional metamodel, in this case the creation of the metamodel and the optimization search for profiles are performed in a space with a nonlinearly reduced dimension. It significantly simplifies the structure of the neural network, *i.e.*, the calculation of the fitness function within the optimization algorithm is performed faster, results in a more accurate search for the extremum due to a reduction in the number of variables in the new space. However, this approach to the final determination of the EC and MP profiles also involves the procedure of nonlinear backprojection into the original full-factor space. Fourth, at the beginning of the metamodel construction, a computer homogeneous design of the experiment is formed, the main task of which is to create the most favourable conditions for the most accurate approximation of the multidimensional response surface in the general case, which is determined by solving a computationally expensive direct magnetodynamic problem according to the Uzal-Cheng-Dodd-Deeds model [1, 16–18], and accumulating additional *a priori* information about the measurement process provided in the digital form to increase its completeness. Moreover, the completeness of additional *a priori* knowledge can be adjusted in both directions, guided by the obtained accuracy of the profile measurement result. Based on the design of the experiment and using the Uzal-Cheng-Dodd-Deeds eddy current measurement process model, a dataset is generated that can potentially be used as a training set for metamodels on deep neural networks in the full-factor search space. However, to move to the reduced space, the data set is projected by nonlinear kernel Gaussian transformations using Kernel PCA techniques into another auxiliary space of a much higher dimensionality than the primary one, where it can be projected by linear PCA transformations into another coordinate system of a lower dimensionality than the primary one. Moreover, such data manipulations lose a fairly small amount of original information inherent in the full-factor space, and its volume is also adjustable. As a result of these actions, we obtain a vector of the desired subsurface profiles of the EC and MP in the real full-factor primary space.

Solving the inverse problem, as noted above, requires an efficient solution of the direct problem. The analytical solution of the magnetodynamic direct problem is further represented by the well-known Uzal-Cheng-Dodd-Deeds model in matrix formulation in the modified Theodoulidis [19] form, which is obtained under the following assumptions: The electromagnetic field is excited by a cylindrical coil with a rectangular cross-section of finite dimensions and a sinusoidal current I varying with an angular frequency ω. The field is quasi-stationary, *i.e.*, wave processes in the air are neglected. The bias currents in the TO are ignored due to their negligible values compared to the conduction currents. The excitation coil is characterized by a homogeneous current density across the cross-section i_0 and has a number of turns W. The TO is assumed to be conditionally multilayer with L of their discrete readings. The laws of distribution of electrophysical parameters of the TO are considered to be known and previously determined experimentally [16]. The mathematical model was created under the assumptions of linearity, isotropy, and homogeneity of the media. The chosen model is very convenient because of its versatility due to the suitability of representing the TO with an arbitrary number of conditional layers. The geometric model of the direct problem is shown in Fig. 2 [20].

In all regions denoted by Fig. 2, the magnetic vector potential A excited by a point source is described by the Helmholtz partial differential equation written in the cylindrical coordinate system, which is supplemented by boundary conditions:

$$\frac{\partial^2 A}{\partial r^2} + \frac{1}{r} \cdot \frac{\partial A}{\partial r} - \frac{A}{r^2} + \frac{\partial^2 A}{\partial z^2} = \widetilde{k}^2 \cdot A - \mu_0 \cdot I \cdot \delta(r - r_0) \cdot \delta(z - z_0), \tag{1}$$

$$\left[\begin{array}{c} A_0 = A_1 \\ \dfrac{\partial A_0}{\partial z} = \dfrac{1}{\mu_{r1}} \cdot \dfrac{\partial A_1}{\partial z} \end{array} \right]_{z=0} \text{and} \quad \left[\begin{array}{c} A_{t+1} = A_t \\ \dfrac{1}{\mu_{t+1}} \cdot \dfrac{\partial A_{t+1}}{\partial z} = \dfrac{1}{\mu_t} \cdot \dfrac{\partial A_t}{\partial z} \end{array} \right]_{z=-d_t}, \tag{2}$$

where $\widetilde{k}^2 = j \cdot \omega \cdot \mu_r \cdot \mu_0 \cdot \sigma$; $j = \sqrt{-1}$; δ – is the Dirac delta-function; r_0, z_0 – are the coordinates of location of the point source of the electromagnetic field, m; $\mu_0 = 4 \cdot \pi \cdot 10^{-7}$ is the magnetic constant, H/m.

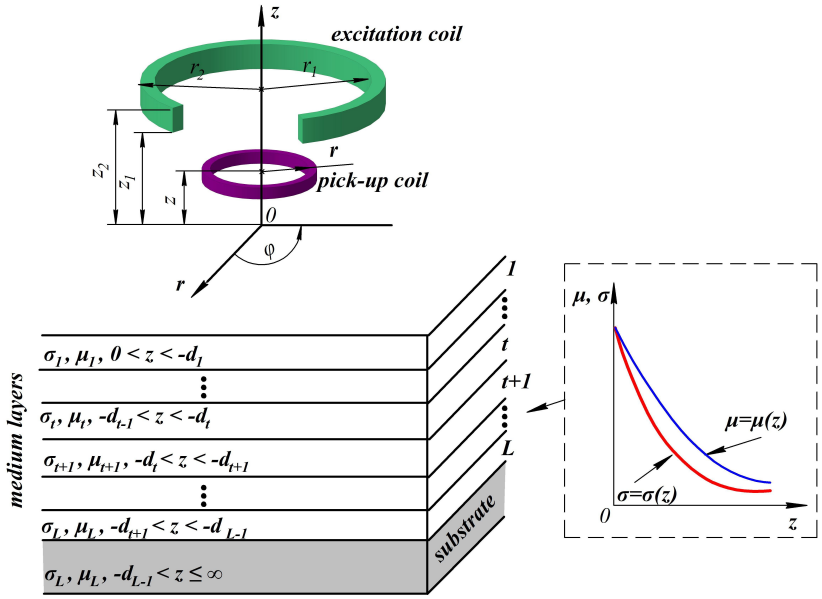

Fig. 2. Geometric model of the direct problem.

Its solution makes it possible to calculate the theoretical model value of the EMF induced in the pick-up coil of the ECP with a radius r and the number of turns w_{mes} by the formula:

$$e_{\text{mod}} = -j \cdot 2 \cdot \pi \cdot r \cdot \omega \cdot w_{\text{mes}} \cdot A_0(P), \tag{3}$$

where

$$A_0 = A^{(s)} + A^{(ec)}; \; A^{(s)} = \int_0^{\infty} J_1(\kappa r) \cdot C_s \cdot e^{\kappa z} d\kappa;$$

$$C_s = \frac{\mu_0 \cdot i_0}{2} \cdot \frac{\chi(\kappa r_1, \kappa r_2)}{\kappa^3} \cdot (e^{-\kappa z_1} - e^{-\kappa z_2});$$

$$\chi(x_1, x_2) = \int_{x_1}^{x_2} x \cdot J_1(x) dx = \left\{ x_1 \cdot J_0(x_1) - 2 \cdot \sum_{m=0}^{\infty} J_{2m+1}(x_1) \right\} - \left\{ x_2 \cdot J_0(x_2) - 2 \cdot \sum_{m=0}^{\infty} J_{2m+1}(x_2) \right\};$$

$$i_0 = W \cdot I \cdot (r_2 - r_1)^{-1} \cdot (z_2 - z_1)^{-1};$$

$$T_{11}(t, t+1) = \frac{1}{2} \cdot e^{(-\lambda_{t+1}+\lambda_t)dt} \cdot \left(1 + \frac{\mu_t}{\mu_{t+1}} \cdot \frac{\lambda_{t+1}}{\lambda_t}\right);$$

$$\mathbf{V} = \mathbf{T}(1,2) \cdot \mathbf{T}(2,3) \ldots \mathbf{T}(L-2, L-1) \cdot \mathbf{T}(L-1, L);$$

$$D_{ec} = \frac{(\kappa \cdot \mu_{t+1} - \lambda_1) \cdot V_{11}(1) + (\kappa \cdot \mu_{t+1} + \lambda_1) \cdot V_{21}(1)}{(\kappa \cdot \mu_{t+1} + \lambda_1) \cdot V_{11}(1) + (\kappa \cdot \mu_{t+1} - \lambda_1) \cdot V_{21}(1)} \cdot C_s;$$

$$T_{12}(t, t+1) = \frac{1}{2} \cdot e^{(\lambda_{t+1}+\lambda_t)dt} \cdot \left(1 - \frac{\mu_t}{\mu_{t+1}} \cdot \frac{\lambda_{t+1}}{\lambda_t}\right);$$

$$T_{21}(t, t+1) = \frac{1}{2} \cdot e^{(-\lambda_{t+1}-\lambda_t)dt} \cdot \left(1 - \frac{\mu_t}{\mu_{t+1}} \cdot \frac{\lambda_{t+1}}{\lambda_t}\right);$$

$$T_{22}(t, t+1) = \frac{1}{2} \cdot e^{(\lambda_{t+1}-\lambda_t)dt} \cdot \left(1 + \frac{\mu_t}{\mu_{t+1}} \cdot \frac{\lambda_{t+1}}{\lambda_t}\right);$$

$$\lambda_t = \left(\kappa^2 + j \cdot \omega \cdot \mu_0 \cdot \mu_t \cdot \sigma_t\right)^{1/2};$$

A_0 is the magnetic vector potential in the air gap below the excitation coil; P is an observation point with coordinates (r, z) belonging to the contour Lc of the ECP measuring coil; $\mathbf{V}$ is a matrix with elements V_{11}, V_{21}; $\mathbf{T}()$ is a matrix with elements $T_{11}()$, $T_{12}()$, $T_{21}()$, $T_{22}()$; $J_m()$ is cylindrical Bessel functions of the first kind of the m-th order; $(r_2 - r_1)$ is the cross-sectional width of the ECP excitation coil, m; $(z_2 - z_1)$ is the height of the cross-section of the ECP excitation coil, m; σ_t and μ_t are the electrophysical properties of the t-th conditional layer of the material.

The adequacy of computer calculations according to formula (3) was proved by comparing with the experimental data given in [21] and the calculated ones obtained using FEM in the COMSOL Multiphysics (AC/DC Module) environment [20] and analytically for two-layer TOs [22].

The problem is that the calculations based on model (3) are resource-intensive, which does not allow its use as part of the fitness function of the optimization algorithm. An effective solution to the direct problem requires the creation of a substitute model, *i.e.*, a metamodel or a model on a model without these drawbacks. The first step in creating a metamodel is to create the design of the experiment with high homogeneity both in general and, most importantly, in all two-dimensional projections. The homogeneous quasi-design was created on modified Sobol's LP_τ -sequences which ensured exactly these properties. More details about the features of the design generation can be found in [23]. The design is made for the full factor space, taking into account the need to introduce additional *a priori* information. The design is a table of size $D \times N$, where D is the number of rows in the table, which is equal to the sum of the number of main and additional factors determining the *a priori* information; N is the number of samples in the training set. However, according to the calculation scheme above, it must be transformed into a reduced space using Kernel PCA techniques [24].

Therefore, we applied a nonlinear projection of the primary data into the auxiliary space using the Gaussian kernel function:

$$\kappa\left(\boldsymbol{x}^{(i)}, \boldsymbol{x}^{(j)}\right) = \exp\left(-\frac{\left\|\boldsymbol{x}^{(i)} - \boldsymbol{x}^{(j)}\right\|^2}{2\theta^2}\right), \tag{4}$$

where θ is a free parameter subject to rational selection; $\boldsymbol{x}^{(i)}$, $\boldsymbol{x}^{(j)}$ is vector-columns of observations of dimension D.

The result of the transformation is a Kernel Matrix $\boldsymbol{K}$ of dimension $N \times N$, *i.e.*, a similarity matrix, where each element is equal to the kernel value between the i-th and j-th observation in the original data.

The structure of this matrix is shown below:

$$\boldsymbol{K} = \begin{bmatrix} \kappa\left(\boldsymbol{x}^{(1)}, \boldsymbol{x}^{(1)}\right) & \kappa\left(\boldsymbol{x}^{(1)}, \boldsymbol{x}^{(2)}\right) & \cdots & \kappa\left(\boldsymbol{x}^{(1)}, \boldsymbol{x}^{(N)}\right) \\ \kappa\left(\boldsymbol{x}^{(2)}, \boldsymbol{x}^{(1)}\right) & \kappa\left(\boldsymbol{x}^{(2)}, \boldsymbol{x}^{(2)}\right) & \cdots & \kappa\left(\boldsymbol{x}^{(2)}, \boldsymbol{x}^{(N)}\right) \\ \vdots & \vdots & \ddots & \vdots \\ \kappa\left(\boldsymbol{x}^{(N)}, \boldsymbol{x}^{(1)}\right) & \kappa\left(\boldsymbol{x}^{(N)}, \boldsymbol{x}^{(2)}\right) & \cdots & \kappa\left(\boldsymbol{x}^{(N)}, \boldsymbol{x}^{(N)}\right) \end{bmatrix}. \tag{5}$$

A symmetric Gram matrix is obtained by centring of a kernel matrix:

$$\widetilde{\boldsymbol{K}} = \boldsymbol{K} - \boldsymbol{1}_N\, \boldsymbol{K} - \boldsymbol{K}\, \mathbf{C}_N + \boldsymbol{1}_N \boldsymbol{K}\, \boldsymbol{1}_N, \tag{6}$$

where $\boldsymbol{1}_N$ is a matrix of size $N \times N$ with elements equal to $1/N$.

The centred matrix is then subjected to a standard linear PCA transformation using the singular value decomposition SVD:

$$\widetilde{\boldsymbol{K}} = \boldsymbol{U}\, \boldsymbol{\Sigma}\, \boldsymbol{U}^T, \tag{7}$$

where $\boldsymbol{U} = \left[\boldsymbol{a}^{(1)}, \ldots, \boldsymbol{a}^{(N)}\right]$ is a matrix containing eigenvectors $\boldsymbol{a}^{(i)} = \left[a_1^{(i)}, \ldots, a_N^{(i)}\right]^T$; $\boldsymbol{\Sigma} = \operatorname{diag}\left(\widetilde{\lambda}_1, \ldots, \widetilde{\lambda}_N\right)$ is a diagonal matrix containing singular numbers whose squares are its eigenvalues.

The first M eigenvectors, selected by ranking in the direction of decreasing eigenvalues $\widetilde{\lambda}_1 \geq \widetilde{\lambda}_2 \geq \ldots \geq \widetilde{\lambda}_N \geq 0$, collect a significant portion of the total variance of the data, while ensuring a negligible loss of information. Thus, such calculations determine the principal components associated with the corresponding M eigenvectors. It is advisable to choose an M much smaller than the dimension of the primary space D. The data of the full-factor design are projected by linear transformations onto the identified principal components, leading to a reduction in dimensionality:

$$\widetilde{\boldsymbol{Z}} = \widetilde{\boldsymbol{U}}^T \widetilde{\boldsymbol{K}}, \tag{8}$$

where $\widetilde{\boldsymbol{U}}^T$ is a reduced matrix of right eigenvectors of dimension $N \times M$.

Therefore, the next step is to build a metamodel of reduced dimensionality of the simplified structure using deep learning. Information on the peculiarities of creating such a metamodel has already been given by the authors in [11, 12]. We only note that, in fact, not one but two real-valued neural network metamodels are created for the real and imaginary parts of the EMF, respectively, and not for their values. Otherwise, we would have to create a complex-valued neural network.

The last stage of computation involves performing surrogate optimization. Important at this stage is the use of a global extremum search algorithm [25, 26], which is fundamental for solving the inverse problem to prevent getting stuck in local minimums of the characteristic complex multidimensional response surface in such cases. To find the extremum of the fitness function in these studies, we used a stochastic metaheuristic hybrid particle swarm global optimization algorithm PSO with evolutionary formation of the swarm composition, which is a low-level hybridization with the genetic algorithm GA. It is characterized by all the properties necessary to solve the inverse problem [27]. The fitness-function was compiled using the least-squares method and minimized by comparing the theoretical modelled ECP signal with the experimental measured value when varying the profiles of the EC and MP.

$$F\left(\boldsymbol{\sigma}, \boldsymbol{\mu}, r, \ldots\right) = \left(\operatorname{Re}\left(e_{\text{mes}}\right) - \operatorname{Re}\left(e_{\text{metamod}}\right)\right)^2 + \left(\operatorname{Im}\left(e_{\text{mes}}\right) - \operatorname{Im}\left(e_{\text{metamod}}\right)\right)^2 \rightarrow \min, \tag{9}$$

where $(\boldsymbol{\sigma}, \boldsymbol{\mu})^T$ is the vector of physical properties of the TO that determines the desired profiles; e_{metamod} is the probe EMF calculated by the reduced dimension metamodel.

The projection into the original space of the solution found by optimization for the Gaussian kernel function chosen in this study is performed by the inverse transformation due to the implementation of the iterative process [28]. The corresponding reconstruction of pre-images for Kernel PCA is implemented by the formula:

$$\boldsymbol{z}^{p+1} = \frac{\sum\limits_{i=1}^{M} \gamma_i k\left(\boldsymbol{z}^p, \boldsymbol{x}^{(i)}\right) \boldsymbol{x}^{(i)}}{\sum\limits_{i=1}^{M} \gamma_i k\left(\boldsymbol{z}^p, \boldsymbol{x}^{(i)}\right)}, \tag{10}$$

where $\gamma_i = \sum\limits_{k=1}^{M} \beta_k a_i^{(k)}$, $i = 1, \ldots, N$; $\beta_k = \sum\limits_{i=1}^{M} a_i^{(k)} k\left(\boldsymbol{x}^{(i)}, \widetilde{\boldsymbol{x}}^*\right)$, $k = 1, \ldots, N$; $\boldsymbol{z}^p$ are the initial values of the vector to initiate the iteration process; $\widetilde{\boldsymbol{x}}^*$ is a vector obtained in the reduced space as a result of optimization; p is the number of the iteration cycle.

The successful execution of the iteration process depends on the successful selection of the vector, which requires careful selection.

Additionally, we note that the mathematical apparatus for solving optimization problems using reduced order surrogate models with all components in the whole, as probated by the authors in [29], demonstrated a fairly high computational efficiency in verifying adequacy on hypothetical test multidimensional mathematical functions with complex topography. Consequently, it can be successfully used to solve inverse measurement problems of determining the material properties profiles of test objects.

Finally, we note that in addition to the main parameters that determine the profiles, the design of experiment additionally included *a priori* information on EMF measurements by coils with different radii r, which provides more efficient information selection than probing of the TO at different excitation frequencies [30–32], although this practice is more common [7, 9, 10].

3. Numerical experiments

Having considered the theoretical foundations, let us proceed to numerical experiments by means of an example, demonstrating the proposed research methodology step by step. First, it is advisable to consider the peculiarities of creating metamodels where the modelling took into account two main factors of electrophysical parameters of the TO and additional *a priori* information on a series of measurements by a coil with different radii r. Then, a homogeneous quasi-experiment design can be implemented on any combination of LP_τ-sequences with the best WSCD values, determined in [33] for the three-factor DOE with subsequent scaling to the required dimensions of the real factor space. Therefore, for example, we used the combination ξ_1, ξ_6, ξ_{14}, with the weighted symmetrized centred divergence index $\text{WSCD} = 8.22856 \cdot 10^{-7}$ for the number of DOE points $N = 2820$. This number of points is sufficient for training deep neural networks with satisfactory accuracy. The table of this DOE on a unit scale is given in [12]. The peculiarities of obtaining of discretized profiles, taking into account the effect of controlled and uncontrolled factors on the TO, are discussed in detail by the authors in [12], so following the recommendations given there for numerical experiments, we set the values of electrophysical properties on the

surface and at the depth of the L-th conditional layer of the TO as follows: $\sigma_L = 2 \cdot 10^6$ S/m, $\sigma_1 = 9.2 \cdot 10^6$ S/m and $\mu_L = 10$, $\mu_1 = 29.78$. Within these limits, the profiles change according to the previously known [16] distribution laws, namely, for example, EC – "exponential", MP – "Gaussian", and the number of conditional layers is taken to be L =60. Then, in particular, taking into account the 15% variation of these parameters [12], we obtain $\sigma_1 = (9.2 \pm 1.38) \cdot 10^6$ S/m, and MP – $\mu_1 = 29.78 \pm 5.25$, with σ_L and μ_L remaining constant at the depth of the material for any sample profiles.

As a result, we obtained a data set in the full factor space, which is shown in Table 1. The next stage involves calculating the model EMF value of the e_{mod} probe at the DOE points using a high-cost magnetodynamic model (3) with the following initial data: for the excitation coil f = 2 kHz, r_1 = 32 mm, r_2 = 50 mm, z_1 =1 mm, z_2 =18 mm, I =1 A, W = 100; for the pick-up coil $r = 6, \ldots, 46$ mm, z = 1 mm, w_{mes} = 50. Some numerical values of this calculation are shown in Table 1.

Table 1. Array of initial data in the full factor space dimension 2820 × (2· L+1).

Profiles	**Parameter**	**Number of the conditional layers**					***r* [mm]**	**ECP signal**	
		1	2	···	59	60		$\text{Re}(e_{\text{mod}})$	$\text{Im}(e_{\text{mod}})$
1	μ	29.750	29.663	···	10.115	10.096	26	–0.8011	1.593
	σ [S/m]	8834221	8486281	···	2092548	2073403			
2	μ	27.129	27.054	···	10.0994	10.083	36	–1.505	3.675
	σ [S/m]	9490569	9110618	···	2128662	2107756			
···	···	···	···	···	···	···	···	···	···
2819	μ	32.405	32.306	···	10.130	10.109	28.27	–0.948	–2.013
	σ [S/m]	9616850	9230741	···	2135611	2114366			
2820	μ	25.852	25.782	···	10.092	10.077	43.2	–1.822	–4.528
	σ [S/m]	9288676	8918572	···	2117553	2097189			

Next, we applied the Kernel PCA method to reduce the dimensionality of the search space [28]. As a result of a number of mathematical transformations, the first 24 eigenvectors with singular numbers greater than 1 were selected (Fig. 3).

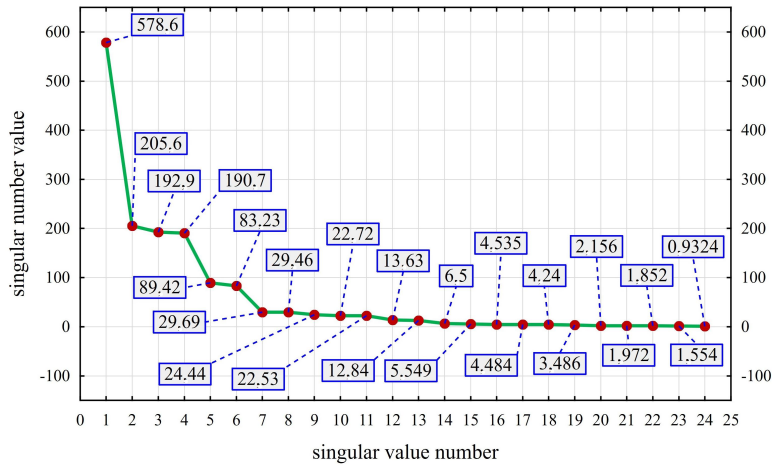

Fig. 3. Diagram of the singular numbers of the Gram matrix.

Thus, we obtained a data matrix that was projected into a reduced space, whose elements are shown in Table 2, which also indicates samples that will be used as training, cross-validation and test samples in the next stage of metamodel construction. Also, those that did not participate in the training and were used later as synthesized samples to verify the reliability of the solution to the inverse profile reconstruction problem. Thus, all the necessary preliminary steps have been taken and a set of initial data (Table 2) has been obtained for building neural network surrogate models using deep ANNs [11, 12, 14, 15, 34].

Table 2. Reduced design matrix of dimension 2820×24 for creating metamodels.

Samples	**Training sample**	**Elements of the reduced design matrix**				
		$\widetilde{Z}^{(1)}$	$\widetilde{Z}^{(2)}$	. . .	$\widetilde{Z}^{(23)}$	$\widetilde{Z}^{(24)}$
1	training	–0.0105	–0.1996	. . .	–0.0339	0.00062519
2		–12.1347	–3.8613	. . .	–0.00099339	–0.0027428
3		12.1315	3.8307	. . .	–0.00099655	–0.0033554
. . .		. . .	. . .	. . .	. . .	. . .
2256		6.1368	–1.1511	. . .	–0.0279	0.0014048
2257	test	–11.1269	4.2567	. . .	–0.0472	–0.0471
. . .		. . .	. . .	. . .	. . .	. . .
2525		12.5145	4.6223	. . .	–0.0012473	0.0167
2526	cross-validation	10.0705	–4.395	. . .	–0.0073356	–0.00099244
. . .		. . .	. . .	. . .	. . .	. . .
2793		13.6944	1.5075	. . .	0.0000021049	–0.0115
2794	verification	0.9098	–2.6965	. . .	0.0479	–0.0017216
. . .		. . .	. . .	. . .	. . .	. . .
2820		–7.7759	–5.2525	. . .	0.0155	0.0137

As a result, neural networks were created for the real and imaginary parts of the EMF separately, the general architecture of which with the specified number of neurons in each hidden layer and their symbols are shown in Fig. 4. At the same time, it should be noted that all hidden layers have a hyperbolic tangent activation function, and the output layer has a linear one. For the imaginary part of the EMF, three neural networks were obtained with errors *MAPE*,% (*Mean Absolute*

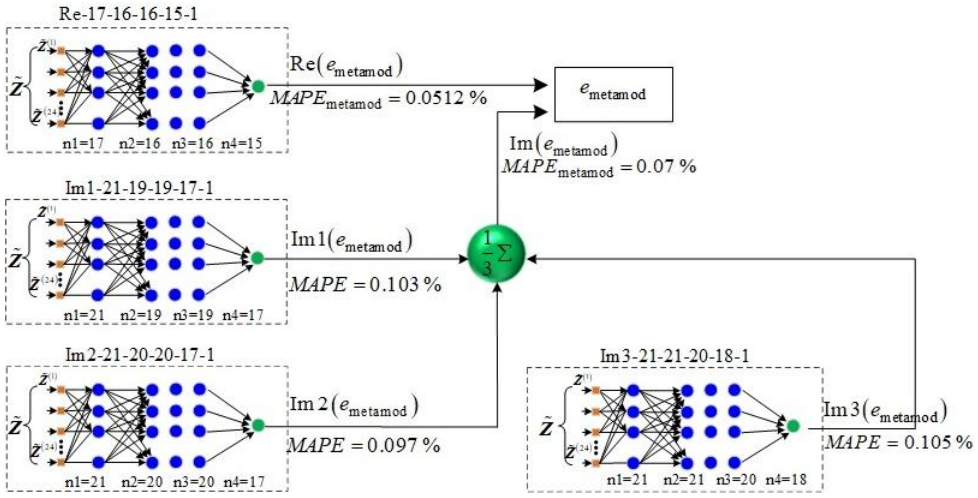

Fig. 4. Architecture of deep neural networks used to build metamodels.

Percentage Error) 0.103, 0.097, 0.105%, respectively. In order to improve the accuracy of the metamodel, ensemble averaging was applied. In result, valid metamodels with low values of the average approximation error $MAPE_{\text{metamod}}$ were built, as shown in Fig. 4.

Both created metamodels are adequate and informative according to Fisher's criterion at the 5% significance level. The coefficient of determination for both of them is R^2 =0.991. Thus, this allows us to proceed to the next stage, namely, to perform the optimization process in the reduced search space. As mentioned above, twenty-six samples were reserved to be used to verify the reliability of the solution to the inverse problem of profile reconstruction. From these data, three samples were selected to perform the procedure for identifying the profiles of the physical properties of the TO (Table 3).

Table 3. Samples for verification of the procedure for determining profiles of electrophysical properties of TO.

Samples		Conditional layers					r [mm]	ECP signal	
		1	2	···	59	60		Re(e_{mes})	Im(e_{mes})
1	$\boldsymbol{\mu}_{\text{ver.}}$	25.135	25.068	···	10.088	10.074	43.66	–1.841	–4.474
	σ_{ver} [S/m]	9857861	9459998	···	2148872	2126980			
2	$\boldsymbol{\mu}_{\text{ver.}}$	25.791	25.721	···	10.092	10.077	21.16	–0.528	–0.876
	σ_{ver} [S/m]	10021950	9616082	···	2157900	2135568			
3	$\boldsymbol{\mu}_{\text{ver.}}$	34.965	34.854	···	10.145	10.122	6.16	–0.041	–0.065
	σ_{ver} [S/m]	9037426	8679576	···	2103729	2084039			

The effectiveness of applying metaheuristic algorithms to a wide class of problems has been shown in [14,23,35–38], and for inverse profile reconstruction problems, the authors demonstrated in it [11,12] using a stochastic metaheuristic hybrid global optimization algorithm. As a result, a set of solution vectors in a reduced space was obtained for each measurement case, the results of which were averaged. By projection, using the iterative inverse Kernel PCA transformation [8], the desired profiles of the physical parameters of the TO in the original space are found. The accuracy of the solution for the verification samples was evaluated by the values of the relative error δ,%, provided that their profiles $\boldsymbol{\mu}_{\text{ver}}$ and σ_{ver} are known (Table 3). Fig. 5 shows a graphical representation of the distributions of relative errors and, additionally, the values of errors *MAPE*,% reproduction of each of the corresponding profiles for the proposed verification measurement samples.

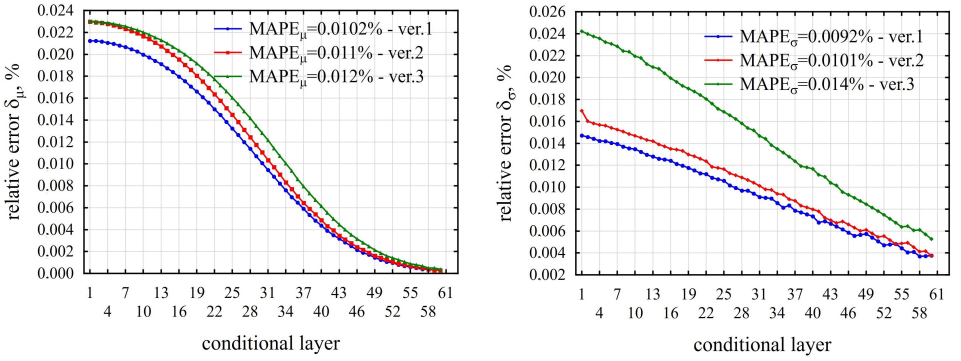

Fig. 5. Graphs of distributions of relative errors of verification measurements of MP profiles (a) and of EC profiles (b).

4. Discussion

Studies similar in methodology, but using the PCA method to reduce the dimensionality of the metamodels, were performed by the authors with *a priori* consideration of the information in the metamodels on various probe excitation frequencies. The results of identifying profiles at excitation frequencies $f = 2 \div 10$ kHz in the reduced space, expressed as maximum errors *MAPE*, were 0.689% for the MP and 0.518% for the EC. In this case, it was possible to reduce the search space to 51% of the original one.

At the same time, model calculations for verification samples in these studies on indirect measurements of electrophysical profiles of planar TOs indicate a greater efficiency of the proposed methodology with Kernel PCA space reduction technology, taking into account additional information on EMF measurements by coils of different radii in metamodels. Here, the obtained values of errors *MAPE*,% for the reconstructed MP profiles are in the range from 0.0102% to 0.012%, and for the EC – from 0.0092% to 0.014%. The reduction of the search space using this method is 80 %, which is a much better result compared to the PCA method used for this purpose.

5. Conclusions

Thus, the study proposes a method for indirect simultaneous measurement of profiles of electrophysical properties of planar objects using the eddy current testing technology, based on the accumulation of additional *a priori* knowledge in digital format in neural network metamodels with nonlinearly reduced dimensionality. The method involves solving an optimization problem by applying a heuristic bionic hybrid algorithm for finding a global extremum using surrogate modelling techniques in a reduced dimension subspace.

The *a priori* accumulation of information is provided in high-performance and low-cost metamodels implemented on the basis of deep fully connected neural networks that take into account, in addition to the electrophysical parameters of the TO, additional information, including incomplete information. At the same time, the accuracy of the created surrogate models, estimated by the errors $MAPE_{\text{metamod}}$ separately for the real and imaginary parts of the EMF, is 0.0512% and 0.07%, respectively.

The use of the Kernel PCA method significantly simplified the conditions for finding an extremum by the optimization algorithm by reducing the number of search variables, which allowed us to move from a 121-dimensional full-factor space to a reduced one with 24 dimensions. The proposed method can be used to assess the quality of various manufacturing processes based on the results of indirect measurements.

Acknowledgements

This work was supported as scientific and research work of Cherkasy State Technological University (Project #0122U200836).

References

[1] Bowler, N. (2019). Eddy-Current Nondestructive Evaluation. In *Springer Series in Measurement Science and Technology*. Springer New York. https://doi.org/10.1007/978-1-4939-9629-2

[2] Sabbagh, H. A., Murphy, R. K., Sabbagh, E. H., Aldrin, J. C., & Knopp, J.S. (2013). Computational Electromagnetics and Model-Based Inversion. In *Scientific Computation*. Springer New York. https://doi.org/10.1007/978-1-4419-8429-6

[3] Liu, G. R., & Han, X. (2003). *Computational Inverse Techniques in Nondestructive Evaluation*. CRC press. https://doi.org/10.1201/9780203494486

[4] Lu, M. (2018). *Forward and Inverse Analysis for Non-destructive Testing Based on Electromagnetic Computation Methods* (Publication No. 10983954) [Doctoral dissertation, University of Manchester]. ProQuest Dissertation & Theses.

[5] Yi, Q., Tian, G. Y., Malekmohammadi, H., Laureti, S., Ricci, M., & Gao, S. (2021). Inverse reconstruction of fibre orientation in multilayer CFRP using forward FEM and eddy current pulsed thermography. *NDT & E International*, *122*, 102474. https://doi.org/10.1016/j.ndteint.2021.102474

[6] Xu, J., Wu, J., Xin, W., & Ge, Z. (2020). Fast measurement of the coating thickness and conductivity using eddy currents and plane wave approximation. *IEEE Sensors Journal*, *21*(1), 306–314. https://doi.org/10.1109/JSEN.2020.3014677

[7] Tesfalem, H., Peyton, A. J., Fletcher, A. D., Brown, M., & Chapman, B. (2020). Conductivity profiling of graphite moderator bricks from multifrequency eddy current measurements. *IEEE Sensors Journal*, *20*(9), 4840–4849. https://doi.org/10.1109/JSEN.2020.2965201

[8] Hampton, J., Fletcher, A., Tesfalem, H., Peyton, A., & Brown, M. (2022). A comparison of non-linear optimisation algorithms for recovering the conductivity depth profile of an electrically conductive block using eddy current inspection. *NDT & E International*, *125*, 102571. https://doi.org/10.1016/j.ndteint.2021.102571

[9] Tesfalem, H., Hampton, J., Fletcher, A. D., Brown, M., & Peyton, A. J. (2021). Electrical resistivity reconstruction of graphite moderator bricks from multi-frequency measurements and artificial neural networks. *IEEE Sensors Journal*, *21*(15), 17005–17016. https://doi.org/10.1109/JSEN.2021.3080127

[10] M. Lu, X. Meng, R. Huang, L. Chen, A. Peyton and W. Yin. (2021). Measuring Lift-Off Distance and Electromagnetic Property of Metal Using Dual-Frequency Linearity Feature. In *IEEE Transactions on Instrumentation and Measurement*, *70*, 1–9, 6001409. https://doi.org/10.1109/TIM.2020.3029348

[11] Halchenko, V. Y., Trembovetska, R., Tychkov, V., Tychkova, N. (2024). Surrogate methods for determining profiles of material properties of planar test objects with accumulation of *a priori* information about them. *Archives of Electrical Engineering*, 183–200. https://doi.org/10.24425/aee.2024.148864

[12] Halchenko, V. Y., Trembovetska, R., Tychkov, V., & Tychkova, N. (2024). Reconstruction of Electrophysical Parameter Distribution During Eddy Current Measurements of Structural Features of Planar Metal Objects. *Latvian Journal of Physics and Technical Sciences*, *61*(3), 61–75. https://doi.org/10.2478/lpts-2024-0021

[13] Kozieł, S., Ogurtsov, S., & Bekasiewicz, A. (2016). Suppressing side-lobes of linear phased array of micro-strip antennas with simulation-based optimization. *Metrology and Measurement Systems*, *23*(2), 193–203. https://doi.org/10.1515/mms-2016-0022

[14] Halchenko, V., Trembovetska, R., Tychkov, V., Sapogov, M., Gromaszek, K., Smailova, S., & Luganskaya, S. (2021). Additive neural network approximation of multidimensional response surfaces for synthesis of eddy-current probes. *Przegląd Elektrotechniczny*, *97*(9), 46–49. https://doi.org/10.15199/48.2021.09.10

[15] Halchenko, V. Y., Trembovetska, R. V., Tychkov, V. V. (2019). Development of excitation structure RBF-metamodels of moving concentric eddy current probe. *Electrical Engineering & Electromechanics*, (2), 28–38. https://doi.org/10.20998/2074-272X.2019.2.05

[16] Uzal, E. (1992). *Theory of Eddy Current Inspection of Layered Metals* (Publication No. 9335046) [Doctoral dissertation, Iowa State University]. ProQuest Dissertation & Theses.

[17] Lei, Y. Z. (2018). General series expression of eddy-current impedance for coil placed above multi-layer plate conductor. *Chinese Physics B*, *27*(6), 060308. https://doi.org/10.1088/1674-1056/27/6/060308

[18] Zhang, J., Yuan, M., Xu, Z., Kim, H. J., & Song, S. J. (2015). Analytical approaches to eddy current nondestructive evaluation for stratified conductive structures. *Journal of Mechanical Science and Technology*, *29*, 4159–4165. https://doi.org/10.1007/s12206-015-0910-7

[19] Theodoulidis, T. P., & Kriezis, E. E. (2006). *Eddy Current Canonical Problems (with Applications to Nondestructive Evaluation)*.

[20] Trembovetska, R., Halchenko, V., & Bazilo, C. (2022, June). Inverse Multi-parameter Identification of Plane Objects Electrophysical Parameters Profiles by Eddy-Current Method. In: *International Conference on Smart Technologies in Urban Engineering*. 202–212. Cham: Springer International Publishing. https://doi.org/10.1007/978-3-031-20141-7_19

[21] Dodd C. V., Deeds W. E. (1975). *Calculation of magnetic fields from time-varying currents in the presence of conductors* (No. ORNL-TM-4958). Oak Ridge National Lab, (ORNL), Oak Ridge, TN (United States).

[22] Halchenko, V. Ya., Trembovetska, R. V., Bazilo, C. V., & Tychkova N. B. (2023). Computer simulation of the process of profiles measuring of objects electrophysical parameters by surface eddy current probes. In *Lecture Notes on Data Engineering and Communications Technologies*: Proceedings of ITEST 2022, 178, 411–424. Springer Cham. https://doi.org/10.1007/978-3-031-35467-0_25

[23] Halchenko, V. Y., Trembovetska, R., Tychkov, V. (2021). Surrogate synthesis of frame eddy current probes with uniform sensitivity in the testing zone. *Metrology and Measurement Systems*, *28*(3). 551–564 https://doi.org/10.24425/mms.2021.137128

[24] Raschka, S., & Mirjalili, V. (2019). *Python Machine Learning: Machine Learning and Deep Learning with Python, scikit-learn, and TensorFlow 2*. 3rd Edition, Packt publishing Ltd.

[25] Li, X., Jia, J., Yang, D., & Gu, Y. (2024). An integration method of a hybrid genetic algorithm and the Levenberg–Marquardt algorithm for ultrasonic testing. *Metrology and Measurement Systems*, *31*(1), 165–177. https://doi.org/10.24425/mms.2024.148536

[26] Yang, X., Cui, Y., Jia, L., Sun, Z., Zhang, P., Zhao, J., & Wang, R. (2023). Parameter identification of PMSM based on dung beetle optimization algorithm. *Archives of Electrical Engineering*, *72*(4). 1055–1072. https://doi.org/10.24425/aee.2023.147426

[27] Halchenko, V. Y., Yakimov, A. N., & Ostapuschenko, D. L. (2010). Global optimum search of functions with using of multiagent swarm optimization hybrid with evolutional composition formation of population. *Information Technology*, *10*, 9–16.

[28] Wang, Q. (2012). Kernel principal component analysis and its applications in face recognition and active shape models. *arXiv preprint arXiv*:1207.3538. https://doi.org/10.48550/arXiv.1207.3538

[29] Halchenko, V., Trembovetska, R., Tychkov, V. (2024). Application of Reduced Order Surrogate Models for Solving Inverse Problems by the Optimization Method with *a priori* Information Accumulation. In: Faure, E., *et al.* Information Technology for Education, Science, and Technics. ITEST 2024. *Lecture Notes on Data Engineering and Communications Technologies*, *222*, 127–142. Springer, Cham. https://doi.org/10.1007/978-3-031-71804-5 _9

[30] Teterko, A. Y., & Gutnik, V. I. (2010). The concept of constructing equipment for multi-parameter eddy current monitoring. Selection and processing of information: *Interdepartmental Collection of Scientific Papers*, *33*(109), 9–14. http://dspace.nbuv.gov.ua/handle/123456789/16217

[31] Teterko, A. Y., & Hutnyk, V. I. (2011). Construction of the inverse transformation function for eddy current multiparameter testing devices. *Materials Science*, *47*, 386–392. https://doi.org/10.1007/s11003-011-9407-4

[32] Teterko, A. Y., & Nazarchuk, Z. T. (2004). Selective Eddy Current Flaw Detection. Karpenko Physicomechanical Institute, Ukrainian Academy of Sciences, Lviv.

[33] Halchenko, V., Trembovetska, R., Tychkov, V., & Tychkova, N. (2023). Construction of Quasi-DOE on Sobol's Sequences with Better Uniformity 2D Projections. *Applied Computer Systems*, *28*(1), 21–34. https://doi.org/10.2478/acss-2023-0003

[34] Halchenko, V. Y., Trembovetska, R. V., & Tychkov, V. V. (2021). Surrogate synthesis of excitation systems for frame tangential eddy current probes. *Archives of Electrical Engineering*, *70*(4), 743–757. https://doi.org/10.24425/aee.2021.138258

[35] Kuznetsov B. I., Nikitina T. B., Bovdui I. V., Chunikhin K. V., Kolomiets V. V., Kobylianskyi B. B. (2024). Method for prediction and control by uncertain microsatellite magnetic cleanliness based on calculation and compensation magnetic field spatial harmonics. *Electrical Engineering & Electromechanics,* (1), 23–33. https://doi.org/10.20998/2074-272X.2024.1.04

[36] Kuznetsov B. I., Kutsenko A. S., Nikitina T. B., Bovdui I. V., Chunikhin K. V., Voloshko O. V. (2024). Hybrid Active and Passive Cable Contour Shielding of Magnetic Fields of Double-Circuit Overhead Power Lines. *Problemele Energeticii Regionale*, *62*(2), 14–27. https://doi.org/10.52254/1857-0070.2024.2-62.02 (in Russian)

[37] Koshevoy, N. D., Muratov, V. V., Kirichenko, A. L., & Borisenko, S. A. (2021). Application of the "jumping frogs" algorithm for research and optimization of the technological process. *Radio Electronics, Computer Science, Control*, *1*(1), 57–65. https://doi.org/10.15588/1607-3274-2021-1-6

[38] Koshevoy, N. D., Kostenko, E. M., & Muratov, V. V. (2020). Application of the fish searñh method for optimization plans of the full factor experiment. *Radio Electronics, Computer Science, Control*, (2), 44–50. https://doi.org/10.15588/1607-3274-2020-2-5

Volodymyr Ya. Halchenko received the Doctor Tech. Sc. degree from Kharkiv State Polytechnic University, Ukraine, in 1999. He is currently Full Professor at the Department of Instrumentation, Mechatronics and Computer Technologies of Cherkasy State Technological University. He has authored or coauthored over 356 publications. He is a member of the Ukrainian Society of Non-Destructive Testing and Technical Diagnostics. His current research interests include non-destructive testing, mathematical modelling, optimization and intellectual data analysis.

Volodymyr Tychkov received the Cand. Tech. Sc. degree from Cherkasy State Technological University, Ukraine in 2017. He is Associate Professor at the Department of Instrumentation, Mechatronics and Computer Technologies of Cherkasy State Technological University. He has authored or coauthored over 291 publications. He is a member of the Ukrainian Society of Non-Destructive Testing and Technical Diagnostics and Full Academic of the Ukrainian Academy of Engineering Sciences. His current research interests include non-destructive testing, mathematical modelling, optimization and intellectual data analysis.

Ruslana Trembovetska received the Doctor Tech. Sc. degree from Cherkasy State Technological University, Ukraine in 2021. She is Professor at the Department of Instrumentation, Mechatronics and Computer Technologies of Cherkasy State Technological University. She has authored or coauthored over 382 publications. She is currently a member of the Ukrainian Society of Non-Destructive Testing and Technical Diagnostics. Her current research interests include non-destructive testing, mathematical modelling, optimization and intellectual data analysis.